Nanoparticle Self-Assembly

DOI: 10.1002/ange.201209304

Size-Dependent Electrostatic Chain Growth of pH-Sensitive Hairy Nanoparticles**

Haibing Xia, Ge Su, and Dayang Wang**

Herein, we demonstrate that stepwise tuning of the environmental pH value can guide the reversible self-assembly of gold nanoparticles (Au NPs) coated with pH-responsive polymer brushes into linear chains. The lengths of the as-prepared NP chains are determined by the environmental pH value. The lengths of chains derived from differently sized NPs at a given pH value are almost identical, whereas the number of NPs per chain is inversely proportional to the NP size. Stepwise tuning of the pH value also enables the integration of differently sized NP chains into composite chains: mesoscopic analogues of block copolymers. In these composite chains, the coupling configurations are strongly dictated by the large/small NP size ratio. NP self-assembly provides an experimentally accessible playground for the detailed study of the association processes of atoms, ions, and molecules, such as the glass transition, crystallization, and condensation polymerization.[1] It also promises an unprecedented approach to the creation of new advanced materials with unusual collective physicochemical properties programmed by the spatial configurations of neighboring NPs.[2,3] For example, inorganic NP chains can exhibit polymer-like properties with respect to their elasticity and their response to external stimuli.[3]

A variety of new synthetic strategies and especially strategies for regioselective surface modification have been developed for the production of NPs with tailored patchy structures and surface chemistry; these features can be harnessed as nanoscale valency to tailor the spatial configuration of neighboring NPs during self-assembly.[4] In parallel to the progress made in the synthesis of anisotropic and/or patchy NPs, a number of studies have underlined the ability of weak interparticle interactions to promote the anisotropic self-assembly of NPs.[5–10] Dipolar interactions can directly or indirectly guide the self-assembly of NPs into chains.[5,6] Some isotropic interactions, such as electrostatic repulsion, can act in an anisotropic manner and thus facilitate the self-assembly of NPs into linear or branched chains.[7] The weak interactions between constituent entities are known to be dependent on the sizes (or mass) of the entities.[11] This size dependence has been found to have a noticeable influence on the morphology of the self-assembled molecules and macromolecules (at least for low-molecular-mass assemblies).[12] In terms of their molecular mass, NPs are (bulky) macromolecules. To date, however, the size dependence of NP self-assemblies has rarely been studied experimentally, although size dependence has drawn increasing interest in the theoretical modeling of the organization behavior of biomacromolecular counterparts, such as proteins and viruses.[13] To address this issue, we studied the electrostatic chain growth of differently sized Au NPs coated with pH-sensitive polymer brushes both experimentally and theoretically.

Monodisperse, quasispherical, citrate-stabilized Au NPs with sizes of (12 ± 1), (25 ± 3), and (36 ± 3) nm were synthesized by the Ag(I)-assisted reduction of $HAuCl_4$ with citrate in boiling water (see Figure S1 in the Supporting Information).[14] Their highly uniform size and sphericity minimized the shape effect on the self-assembly of the NPs. The Au NPs were then coated with pH-sensitive polymer brushes, poly{[2-(dimethylamino)ethyl] methacrylate} (PDMA), and with PDMA complexed with disodium citrate (termed C-PDMA) by ligand exchange to form Au_m@PDMA and Au_m@C-PDMA NPs, respectively, in which m is the diameter of the Au cores (see the Supporting Information for experimental details).[15] The Au_m@PDMA NPs were positively charged (ζ potential >25 mV) at pH <7.0 as a result of protonation of the PDMA brushes anchored on the NPs ($pK_a=7.0$[16]; see Figure S2). When the pH value of the medium increased above 7.0, deprotonation of the PDMA brushes made the NPs become hydrophobic; above pH 13, the NPs agglomerated randomly and eventually precipitated (see Figure S3). In contrast, at pH >4.0, the Au_m@C-PDMA NPs had a ζ potential of -35 mV, which is slightly larger than that of original citrate-stabilized NPs (-45 mV; see Figure S4). This ζ potential indicates that the citrate rather than PDMA dictated the charge character of the C-PDMA NP coating. When the pH value of the medium was adjusted stepwise to below the smallest pKa value of citrate (3.2[17]), the Au_m@C-PDMA NPs remained considerably negatively charged: the ζ potential increased from -35 to -33, -30, and -15 mV when the pH value was decreased from 4.0 to 3.5, 3.0, and 2.5 (see Figure S4). When the pH value was decreased (Figure 1a), the surface plasmon resonance (SPR) band of the Au_{12}@C-PDMA NPs, originally centered at 520 nm, became noticeably weaker; at the same time, the

[*] Prof. H. Xia
State Key Laboratory of Crystal Materials, Shandong University
Jinan, 250100 (P. R. China)
E-mail: xia@icm.sdu.edu.cn
G. Su, Prof. D. Wang
Ian Wark Research Institute, University of South Australia
Adelaide, SA 5095 (Australia)
E-mail: dayang.wang@unisa.edu.au

[**] H.X. is grateful to the Natural Science Foundation of China (51002086, 51172126, and 51021062) and the 973 Program (2010CB630702) for financial support. This research was also supported by NCET (2010) and the IIFSDU (2010JQ013). D.W. thanks the Australian Research Council for financial support (DP 110104179 and DP 120102959).

Supporting information for this article is available on the WWW under http://dx.doi.org/10.1002/anie.201209304.

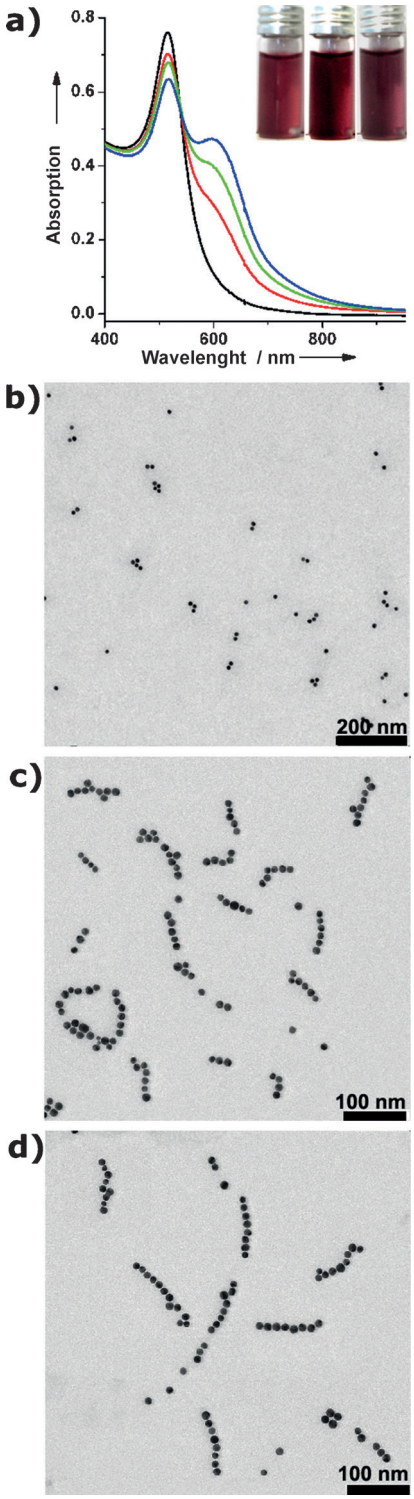

Figure 1. a) Evolution of the absorption spectrum of an aqueous dispersion of Au_{12}@C-PDMA NPs as the pH value of the medium was decreased from 4.0 (black curve) to 3.5 (red curve), 3.0 (green curve), and 2.5 (blue curve). The inset shows photographs of the dispersion at pH 3.5 (left), 3.0 (middle), and 2.5 (right). b–d) TEM images of Au_{12}@C-PDMA NP chains obtained at pH 3.5 (b), 3.0 (c), and 2.5 (d).

absorption tail at wavelengths above 600 nm was gradually red shifted and eventually evolved into a pronounced band centered at 640 nm. In accompaniment with the change in the spectral profile, the color of the NP dispersion changed from red to dark purple (inset in Figure 1 a). Transmission electron microscopy (TEM) imaging confirmed the formation of linear Au_{12}@C-PDMA NP chains; the number of NPs per chain increased from 2 ± 1 (Figure 1 b) to 5 ± 1 (Figure 1 c) and 8 ± 1 (Figure 1 d) as the pH value was decreased stepwise to 3.5, 3.0, and 2.5. Accordingly, one can assign the new absorption band above 600 nm (Figure 1 a) to transverse plasmon electron coupling of neighboring Au cores in the NP chains.[7b] An isosbestic point present in the absorption spectra (Figure 1 a) highlights that only single NPs and newly formed NP chains existed in the NP dispersions as the pH value was decreased.

After the pH value of the medium had been adjusted to a given value, there was little change in the absorption spectrum of the dispersion of as-prepared Au_{12}@C-PDMA NP chains after 10 min (see Figure S5); precipitation of the as-prepared chains was hardly visible for least a month. Thus, the as-prepared Au_{12}@C-PDMA NP chains showed good colloidal and structural stability. When the pH value of the medium was below 2.5, the NPs became weakly charged (ζ potential > -12 mV; see Figure S4), and branched-chain networks were formed and gradually precipitated (see Figure S6). This behavior suggests that the growth of the NP chains and their colloidal stability are dictated mainly by electrostatic repulsion rather than by the steric repulsion induced by the C-PDMA brushes, as steric repulsion is expected to be less pH-sensitive owing to the excellent hydration of citrate even in the protonated form at pH < 3.2 (its lowest pK_a value). On the other hand, the good structural stability and reasonably narrow length distribution of the as-prepared Au_{12}@C-PDMA NP chains imply that the growth of the NP chains is a thermodynamically controlled process, since a broad length distribution and structural evolution would be expected for a kinetically controlled assembly process.[1c,e]

As suggested previously,[7b,c] the electrostatic repulsion (V_{ER}^{end}) between single NPs and the ends of growing NP chains is always smaller than that between the NPs and the sides of the NP chains, and the chain growth of charged NPs can be regarded as a result of the balance between this electrostatic repulsion and the attraction (V_{A}^{end}) (in this case hydrogen bonding (V_{HB}^{end}) plus van der Waals interactions (V_{VdW}^{end})) between the ends of growing NP chains and single NPs. The term V_{ER}^{end} can be described by Equation (1):[7b]

$$V_{ER}^{end} = \sum_{n} \frac{Q}{l_i} = \int_{0}^{D_{total}} \frac{\rho S}{l_i} dl = \rho A \ln l_{total} = \rho A \ln nd \qquad (1)$$

in which Q, ρ, and S are the effective surface charge, surface charge density, and surface area, respectively, of NPs with diameters D, and l_{total} is the length of the NP chain comprising n ($n > 2$) NPs. At the equilibrium of NP chain growth, V_{ER}^{end} is equal to V_{A}^{end}, so l_{total} can be described simply by Equation (2):

$$l_{total} = nd = \exp[(-V_{A}^{end})/\rho S] \qquad (2)$$

Since $S=\pi d^2$, Equation (2) can be expressed as follows:

$$l_{\text{total}} = nd = 1 + \frac{[6(-V_A^{end})/\rho\pi]}{d^2} + \frac{[6(-V_A^{end})/\rho\pi]^2}{2!d^4} + \frac{[6(-V_A^{end})/\rho\pi]^3}{3!d^6} + \ldots \quad (3)$$

The term V_{HB}^{end} ought to increase with the number of hydrogen donors (hydrogen atoms) and hydrogen acceptors (oxygen or nitrogen atoms) on the NPs and thus with the surface area, S, of the NPs $\left(V_{HB}^{end} \propto d^2\right)$. The term V_{VdW}^{end} is correlated with the diameter, d, of the starting NPs according to the equation $V_{VdW}^{end} = -A\,d/6x$, in which A is the Hamaker constant and x is the distance between the NP surfaces. According to Equation (3), therefore, the length of the NP chain, l_{total}, should weakly depend on the diameter of the NPs. On the other hand, n should be inversely proportional to the diameter of the starting NPs as described by Equation (4):

$$n = \frac{1}{d} + \frac{[6(-V_A^{end})/\rho\pi]}{d^3} + \frac{[6(-V_A^{end})/\rho\pi]^2}{2!d^5} + \frac{[6(-V_A^{end})/\rho\pi]^3}{3!d^7} + \ldots \quad (4)$$

To validate the size dependence of electrostatic NP-chain growth, the reversible self-assembly of Au_{25}@C-PDMA and Au_{36}@C-PDMA NPs into chains was guided by stepwise adjustment of the pH value in the range of 2.5–4.0 (Figure 2; see also Figure S7). With a size increase of the Au NP cores from 12 to 25 and 36 nm (the C-PDMA shell thickness is 5 nm for all NPs), the n value of the as-prepared Au_m@C-PDMA NP chains decreased from 5 ± 1 (Figure 1c) to 3 ± 1 (Figure 2a) and 2 ± 1 (Figure 2c) for NP chains obtained at pH 3.0, and from 8 ± 1 (Figure 1d) to 6 ± 1 (Figure 2b) and 3 ± 1 (Figure 2d) for NP chains obtained at pH 2.5. The l_{total} values were comparable for three different Au_m@C-PDMA NP chains formed at a given pH value when the fact that a small variation in n causes a large deviation in l_{total}, especially for large NPs, is taken into account: the l_{total} values were about 70–140 nm at pH 3.0 and 130–220 nm at pH 2.5. These data are consistent with the predictions of Equation (3) and Equation (4).

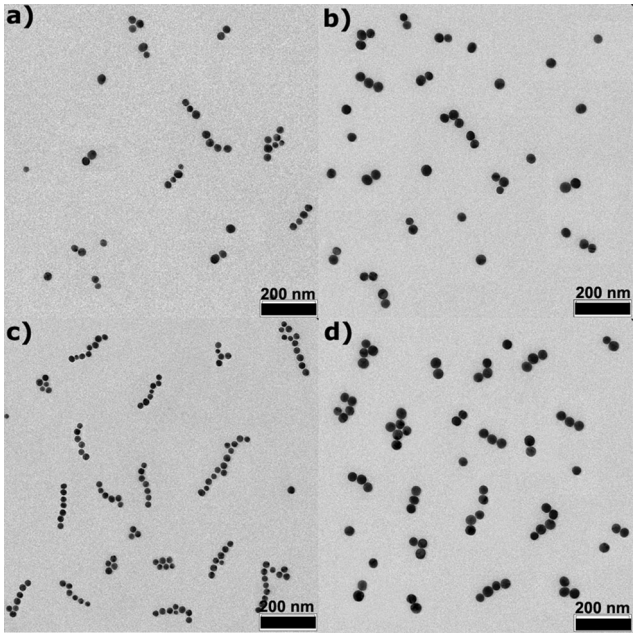

Figure 2. TEM images of a,b) Au_{25}@C-PDMA and c,d) Au_{36}@C-PDMA NP chains obtained at pH 3.0 (a and c) and 2.5 (b and d).

External stimuli can often be used to direct the reversible agglomeration of NPs in dispersions.[18] Wang and co-workers demonstrated the reversible pH-induced chain growth of gold nanorods by the appropriate selection of bifunctional thiols as coupling agents.[18a] In this study, we observed that when the pH value of the medium was adjusted in a stepwise manner back to 4.0 to recharge the C-PDMA coating and thus increase the electrostatic repulsion between the NPs in as-prepared Au_{12}@C-PDMA NP chains, the transverse SPR band centered at 640 nm gradually disappeared, and the longitudinal SPR band centered at 520 nm was significantly enhanced (see Figure S8a). The NP chains dissociated into single NPs after about 25 min upon incubation at pH 4 (see Figure S8c). The resulting single NPs readily reassembled into chains when the pH value was decreased from 4.0. The lengths and spectral profiles of the resulting chains were almost identical to those of the initial NP chains (see Figure S9). The observed reversibility of the pH-induced chain growth of Au_{12}@C-PDMA NPs first suggests that the adjacent NPs in the resulting NP chains are coupled mainly through hydrogen bonding of their pronated C-PDMA brushes. Second, it suggests that the van der Waals attraction between adjacent NPs is offset by the steric repulsion induced by their C-PDMA brushes. This effect is plausible, as the hydrodynamic thickness of the C-PDMA-brush shells was measured as 5 nm by dynamic light scattering. After the complete dissociation of the as-prepared NP chains at pH > 4.0, however, a non-negligible amount of NP dimers and trimers were observed (see Figure S8c). The formation of dimers and trimers was also evidenced by a noticeable absorption at wavelengths above 600 nm in the absorption spectra of the resulting NP dispersions (see Figure S8a) and is probably due to the inevitable dissipation of C-PDMA brushes in the close-contact region between neighboring NPs in the chains.[7b,8] When NP chain growth and dissociation were repeated 2 or 3 times, the existence of a small amount of NP dimers or trimers had little influence on either the length or the absorption spectral profile of the resulting NP chains (see Figure S9). This result implies that the electrostatic-repulsion-driven chain growth of NPs is reasonably tolerant toward the size and shape of the NPs.

Encouraged by the reversibility and pH dependence of the electrostatic chain growth of Au_m@C-PDMA NPs, we tested the possibility of stitching together two NP chains of different sizes by stepwise adjustment of the pH value (see the Supporting Information for experimental details). We succeeded in the end-to-end coupling of Au_{25}@C-PDMA NP (3 ± 1 NPs per chain) and Au_{36}@C-PDMA chains (2 ± 1 NPs per chain) formed at pH 3.0 to give linear composite chains by decreasing the pH value of a dispersion of the two chain types from 3.0 to 2.5 (Figures 3a; see also Figure S10a). Figure 3b summarizes the different coupling configurations of the linear composite chains prepared from Au_{25}@C-PDMA and

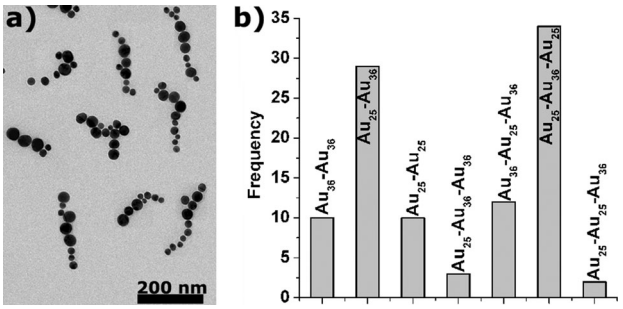

Figure 3. a) TEM image of linear composite NP chains obtained by the coupling of as-prepared Au_{25}@C-PDMA and Au_{36}@C-PDMA NP chains. b) Distribution of the resulting linear composite NP chains with different coupling configurations.

Au_{36}@C-PDMA NP chains: Au_{25}–Au_{25}, Au_{36}–Au_{36}, Au_{25}–Au_{36}, Au_{25}–Au_{25}–Au_{36}, Au_{25}–Au_{36}–Au_{25}, Au_{25}–Au_{36}–Au_{36}, and Au_{36}–Au_{25}–Au_{36}. Intriguingly, the dominant populations are block-copolymer-like chains: Au_{25}–Au_{36} (ca. 30%), Au_{25}–Au_{36}–Au_{25} (ca. 35%), and Au_{36}–Au_{25}–Au_{36} (ca. 12.5%), whereas randomly mixed chains, Au_{25}–Au_{25}–Au_{36} and Au_{25}–Au_{36}–Au_{36}, accounted for less than 2.5% of the chains formed. Self-coupled populations are non-negligible: Au_{25}–Au_{25} (ca. 10%) and Au_{36}–Au_{36} (ca. 10%). Since about three times as much of the chain type Au_{25}–Au_{36}–Au_{25} (ca. 35%) was formed than Au_{36}–Au_{25}–Au_{36} (ca. 12.5%), the ends of the Au_{36}@C-PDMA NP chains appear to be more attractive than those of the Au_{25}@C-PDMA NP chains; otherwise, the latter population would be dominant. This property is probably due to the large longitudinal dimension (the NP diameters) of Au_{36}@C-PDMA NPs, which leads to stronger V_{HB}^{end} and V_{VdW}^{end} values, as mentioned above. When preformed Au_{12}@C-PDMA NP chains were mixed with either preformed Au_{25}@C-PDMA or preformed Au_{36}@C-PDMA chains, however, end-to-end chain coupling was hardly observed at all; instead, coupling of the chains of small NPs to the sides of the chains of large NPs tended to occur (see Figure S11).

To rationalize the revealing effect of the large/small NP size ratio on the coupling configuration of as-prepared composite NP chains, we analyzed the interaction balance during the coupling of chains composed of small and large NPs. Since both small and large NPs and their chains were reasonably stable and they were coupled together dominantly in the end-to-end and/or end-to-side configurations, side-to-side coupling was not taken into consideration. For the sake of simplification, hydrogen bonding between chains composed of small and large NPs was also ignored; the extent of hydrogen bonding should be determined mainly by the longitudinal dimension (the NP diameters) of the chains of large NPs and should be less dependent on the NP size ratio. At the equilibrium of the coupling of chains of small NPs with chains of large NPs to form linear composite chains, therefore, the end-to-end electrostatic repulsion $\left({}^{SL}V_{ER}^{E-E}\right)$ simply equals the end-to-end van der Waals attraction $\left({}^{SL}V_{VdW}^{E-E}\right)$, ${}^{SL}V_{VdW}^{E-E} \approx {}^{SL}V_{ER}^{E-E}$. To prevent end-to-side NP-chain coupling, on the other hand, the end-to-side electrostatic repulsion $\left({}^{SL}V_{ER}^{E-S}\right)$, assumed to be $2^{SL}V_{ER}^{E-E}$,[7b] should be equal to or larger than the end-to-side van der Waals attraction $\left({}^{SL}V_{VdW}^{E-S}\right)$. Thus, one can obtain:

$$ {}^{SL}V_{VdW}^{E-S}/{}^{SL}V_{ER}^{E-S} = {}^{SL}V_{VdW}^{E-S}/2^{SL}V_{ER}^{E-E} = {}^{SL}V_{VdW}^{E-S}/2^{SL}V_{VdW}^{E-E} \leq 1 \quad (5)$$

Herein, ${}^{SL}V_{VdW}^{E-E}$ is simplified as the van der Waals attraction between small NPs with diameters d_S and large NPs with diameters d_L:[11]

$$ {}^{SL}V_{VdW}^{E-E} = -\frac{A}{12x}\frac{d_S d_L}{d_S + d_L} \quad (6)$$

${}^{SL}V_{VdW}^{E-S}$ is simply calculated as the van der Waals attraction between two crossed cylinders:[11]

$$ {}^{SL}V_{VdW}^{E-S} = -\frac{A}{12x}\sqrt{d_S d_L} \quad (7)$$

Thus, Equation (5) can be expressed as follows:

$$ {}^{SL}V_{VdW}^{E-S}/{}^{SL}V_{VdW}^{E-E} = (d_S + d_L)\Big/\sqrt{d_S d_L} = \sqrt{r} + \frac{1}{\sqrt{r}} \leq 2 \quad (8)$$

in which $r = d_L/d_S$. Clearly, Equation (8) can be satisfied only when $r = 1$, which underlines the risk of random coupling upon the mixing of differently sized NP chains. In the current study, on the other hand, the polymer coating of Au_m@C-PDMA NPs provides steric repulsion (${}^{SL}V_{ST}$) to stabilize the NPs and their chains in addition to electrostatic repulsion. By incorporating ${}^{SL}V_{ST}$ into Equation (5), Equation (8) can then be described as follows:

$$ \sqrt{r} + \frac{1}{\sqrt{r}} \leq 2 + C \quad (9)$$

in which $C = {}^{SL}V_{ST}/{}^{SL}V_{ER}^{E-E}$. For a given thickness of the polymer coating, ${}^{SL}V_{ST}$ is dependent on the diameter of the NPs. Herein, ${}^{SL}V_{ST}$ is simply calculated as the steric repulsion between small NPs to reveal the critical value of r for end-to-end coupling of chains of small NPs with chains of large NPs. C was calculated to be 0.06 for Au_{25}@C-PDMA NPs, and r must have a value of 1.64 or less, according to Equation (9), for Au_{25}@C-PDMA NP chains to undergo end-to-end coupling with chains of large NPs. In the case of the coupling of Au_{25}@C-PDMA and Au_{36}@C-PDMA NP chains, $r \leq 1.31$, so the growth of linear composite chains is thermodynamically favorable. C was calculated to be 0.05 for Au_{12}@C-PDMA NPs, and r must have a value of 1.55 or less, according to Equation (9), for Au_{12}@C-PDMA NP chains to undergo end-to-end coupling with large NP chains. In the case of the coupling of Au_{12}@C-PDMA NP chains with Au_{25}@C-PDMA or Au_{36}@C-PDMA NP chains, $r = 1.59$ or $r = 2.09$, so end-to-end coupling is not favorable, and end-to-side coupling is unavoidable. The size-ratio effect on the coupling of as-prepared NP chains, as predicted by our coarse model, is quite consistent with the report of Chen and co-workers on the coassembly of small and large NPs into composite NP chains.[7c]

In summary, we have demonstrated that pH-sensitive hairy Au_m@C-PDMA NPs can reversibly self-assemble into

chains in response to the stepwise adjustment of the environmental pH value, and that their self-assembly is driven mainly by the pH-dependent electrostatic repulsions between the NPs. The length of as-prepared NP chains is determined by the environmental pH value and depends little on the size of the NPs, whereas the number of NPs per chain decreases as the NP size increases. We have also succeeded in the coupling of as-prepared differently sized NP chains to form linear composite chains with configurations reminiscent of those of di- or triblock copolymers; however, the configuration of the composite chains is strongly dependent on the large/small NP size ratio. The dependence of NP-chain growth on the size of the NPs and the size ratio of NPs of different sizes has been rationalized by analysis of the balance of the interactions between the NPs, between the NP chains, and between the NPs and the NP chains. The statistics established for the size dependence of NP-chain growth and the size-dependent coupling configuration of these chains should make the present chain growth of pH-sensitive hairy NPs a better model for the study of molecular-association processes, such as protein synthesis[19] and organization.[13] The resulting Au NP homo- and heterochains with defined but varied lengths and coupling configurations provide a new class of mesoscopic plasmonic polymers,[20] which may hold immense promise in nanotechnology.

Received: November 21, 2012
Revised: January 22, 2013
Published online: February 18, 2013

Keywords: gold · nanoparticles · pH response · self-assembly · size effects

[1] a) W. Irvine, V. Vitelli, P. Chaikin, *Nature* **2010**, *468*, 947 – 951; b) G. A. DeVries, M. Brunnbauer, Y. Hu, A. M. Jackson, B. Long, B. T. Neltner, O. Uzun, B. H. Wunsch, F. Stellacci, *Science* **2007**, *315*, 358 – 361; c) K. Liu, Z. Nie, N. Zhao, W. Li, M. Rubinstein, E. Kumacheva, *Science* **2010**, *329*, 197 – 200; d) H. Wang, L. Chen, X. Shen, L. Zhu, J. He, H. Chen, *Angew. Chem.* **2012**, *124*, 8145 – 8149; *Angew. Chem. Int. Ed.* **2012**, *51*, 8021 – 8025; e) B. Zhang, W. Zhao, D. Wang, *Chem. Sci.* **2012**, *3*, 2252 – 2256.

[2] F. Sciortino, *Eur. Phys. J. B* **2008**, *64*, 505 – 509.

[3] a) S. K. Friedlander, *J. Nanopart. Res.* **1999**, *1*, 9 – 15; b) M. P. Pileni, *Acc. Chem. Res.* **2008**, *41*, 1799 – 1809.

[4] a) S. C. Glotzer, M. J. Solomon, *Nat. Mater.* **2007**, *6*, 557 – 562; b) Z. Mao, H. Xu, D. Wang, *Adv. Funct. Mater.* **2010**, *20*, 1053 – 1074; c) M. Grzelczak, J. Vermant, E. M. Furst, L. M. Liz-Marzán, *ACS Nano* **2010**, *4*, 3591 – 3605.

[5] P. Akcora, H. Liu, S. K. Kumar, J. Moll, Y. Li, B. C. Benicewicz, L. S. Schadler, D. Acehan, A. Z. Panagiotopoulos, V. Pryamitsyn, V. Ganesan, J. Ilavsky, P. Thiyagarajan, R. H. Colby, J. F. Douglas, *Nat. Mater.* **2009**, *8*, 354 – 359.

[6] K. Butter, P. Bomans, P. Frederik, G. Vroege, A. Philipse, *Nat. Mater.* **2003**, *2*, 88 – 91.

[7] a) S. Lin, M. Li, E. Dujardin, C. Girard, S. Mann, *Adv. Mater.* **2005**, *17*, 2553 – 2559; b) H. Zhang, D. Wang, *Angew. Chem.* **2008**, *120*, 4048 – 4051; *Angew. Chem. Int. Ed.* **2008**, *47*, 3984 – 3987; c) M. Yang, G. Chen, Y. Zhao, G. Silber, Y. Wang, S. Xing, Y. Han, H. Chen, *Phys. Chem. Chem. Phys.* **2010**, *12*, 11850 – 11860.

[8] M. S. Nikolic, C. Olsson, A. Salcher, A. Kornowski, A. Rank, R. Schubert, A. Frömsdorf, H. Weller, S. Förster, *Angew. Chem.* **2009**, *121*, 2790 – 2792; *Angew. Chem. Int. Ed.* **2009**, *48*, 2752 – 2754.

[9] N. Zhao, K. Liu, J. Greener, Z. Nie, E. Kumacheva, *Nano Lett.* **2009**, *9*, 3077 – 3081.

[10] M. Grzelczak, A. Sánchez-Iglesias, H. Heidari Mezerji, S. Bals, J. Pérez-Juste, L. M. Liz-Marzán, *Nano Lett.* **2012**, *12*, 4380 – 4384.

[11] J. Israelachvili, *Intermolecular and Surface Forces*, Academic Press, New York, 2nd ed., **1991**.

[12] a) G. Srinivas, D. E. Discher, M. L. Klein, *Nat. Mater.* **2004**, *3*, 638 – 644; b) B. Zhao, R. T. Haasch, S. MacLaren, *J. Am. Chem. Soc.* **2004**, *126*, 6124 – 6134; c) W. Li, W. Jiang, *Macromol. Theory Simul.* **2009**, *18*, 434 – 440.

[13] T. Chen, Z. Zhang, S. C. Glotzer, *Proc. Natl. Acad. Sci. USA* **2007**, *104*, 717 – 722.

[14] H. Xia, S. Bai, J. Harmann, D. Wang, *Langmuir* **2010**, *26*, 3585 – 3589.

[15] E. W. Edwards, M. Chanana, D. Wang, H. Möhwald, *J. Phys. Chem. C* **2008**, *112*, 15207 – 15219.

[16] X. Chen, D. P. Randall, C. Perruchot, J. F. Watts, T. E. Patten, T. von Werne, S. P. Armes, *J. Colloid Interface Sci.* **2003**, *257*, 56 – 64.

[17] X. Ji, X. Song, J. Li, Y. Bai, W. Yang, X. Peng, *J. Am. Chem. Soc.* **2007**, *129*, 13939 – 13948.

[18] a) Z. Sun, W. Ni, Z. Yang, X. Kou, L. Li, J. Wang, *Small* **2008**, *4*, 1287 – 1292; b) T. Isojima, M. Lattuada, J. B. Vander Sande, T. A. Hatton, *ACS Nano* **2008**, *2*, 1799 – 1806; c) R. Klajn, P. J. Wesson, K. J. M. Bishop, B. A. Grzybowski, *Angew. Chem.* **2009**, *121*, 7169 – 7173; *Angew. Chem. Int. Ed.* **2009**, *48*, 7035 – 7039; d) Y. Liu, X. Han, L. He, Y. Yin, *Angew. Chem.* **2012**, *124*, 6479 – 6483; *Angew. Chem. Int. Ed.* **2012**, *51*, 6373 – 6377.

[19] A. R. Mitchell, *Pept. Sci.* **2008**, *90*, 215 – 233.

[20] L. S. Slaughter, B. A. Willingham, W. C. Chang, M. H. Chester, N. Ogden, S. Link, *Nano Lett.* **2012**, *12*, 3967 – 3972.

